

Passive Turbine-like Mechanical Fan with Turbulence Generator in Low-speed Flow

Arie Sukma Jaya¹, Byan Wahyu Riyandwita², Yose Fachmi Buys³

{arie.sj@universitaspertamina.ac.id¹, byan.wr@universitaspertamina.ac.id²,
yose.fachmi@universitaspertamina.ac.id³}

Department of Mechanical Engineering, Faculty of Industrial Technology, Universitas Pertamina^{1,2,3}

Abstract. A turbine converts the energy of the incoming fluid flow into mechanical energy that is responsible for the electricity generation in wind power and hydropower. The low-speed incoming flow might reduce the performance of the turbine. By creating a turbulence incoming flow, thus increasing the kinetic energy of the flow, the turbine might rotate at a lower threshold of the incoming flow speed. The significance of the turbulence generator was evaluated experimentally by using a turbine-like mechanical fan and a passive turbulence generator in a sinking test in a water tank. The experiments were arranged with a full factorial design method at two levels and three factors of diameter (D_T), maximum length (L_T), and distance of the turbulence generator (s_T). This study suggests that the distance of the turbulence generator (s_T) is the significant factor within the significant level of 0.05, degree of freedom of 4, and t-value of 2.776.

Keywords: Turbulence, Turbine-like, Low-speed, Factorial design, Water tank.

1 Introduction

Electrical machines are related to the conversion between mechanical and electrical energy. The machines are generally classified as motors and generators. Any type of mechanical device that converts the stream energy of fluid into mechanical energy is called a turbine [1]. There are four types of turbines which are water, steam, gas, and wind turbines. Power generation with a turbine is usually coupled with a generator [2]. A turbine that utilizes the wind as the source of the fluid stream is called a wind turbine [3, 4]. In a wind turbine, the speed of the wind should largely determine the amount of electricity generated by the turbine. Higher wind speeds should have a higher kinetic energy of the stream, which in turn increases the mechanical energy to the generator represented by a faster rotational speed of the turbine blades [5]. The higher input of mechanical energy of the generator increases the generated electrical energy in power generation. In this way, it is usually preferable to study the wind speed before the installation of the fluid stream-powered generator.

In the field of flow control, there is a well-known device that enhances the kinetic energy of the fluid stream in the form of a turbulence generator. The device converts an incoming flow of fluid into a turbulent flow [6-9]. Most turbulence generators are simple mechanical devices,

such as those using roughness and helical spring. The roughness method introduces an external surface or object to the observed body. It generates turbulence to delay the flow separation, such as in a golf ball or the wing of an airplane. Another type is the helical spring, such as for flow in the pipe, in which an external helical structure is placed on the surface of a fluid container. This helical structure will introduce a turbulent flow with an increasing flow velocity to the stream, resulting in the higher kinetic energy of the stream. Several studies have been linked between turbulence generators and turbine power generators. The turbine power output was substantially increased in the presence of grid turbulence. The self-starting behavior of the vertical axis wind turbine is improved under the influence of external free-stream turbulence. The integral scale along the rotor axis is found to grow linearly with distance, independent of the incoming turbulence levels [10, 11].

There were many attempts to increase the efficiency of the power generation turbine such as wind turbines [12]. However, there were relatively rare discussions that relate the efficiency of the power generation turbine in a low-speed flow regime to the rotational enhancement of the turbine by using a turbulence generator. How to enhance rotational speed, confirm the significant effect of the turbulence generator, and determine the main factor of the turbulence generator were among the research questions in this work. This study purposely investigates the enhancement of power generation turbine performance in low-speed flow by using a passive turbulence generator. Passive means the turbulence generator is not powered and controlled by any electronic part [13]. Therefore, at first, this study implemented a simple passive turbulence generator to enhance the rotational speed of the turbine blades. Then experimentally measuring the effectiveness of the turbulence generator in increasing the rotational speed of the passive turbine blades. Finally, this study used a factorial design method to determine the significant factor affecting the rotational speed of the passive turbine blades. This study should be considered a preliminary experimental study by employing a factorial design method in the experimental process [14, 15].

2 Experimental setup and procedure

The experimental setup and procedure were developed to accommodate the objective and research question of the study. The initial part of this section describes the simplified model of a turbine using a turbine-like mechanical fan, followed by a brief explanation of the sinking test in a water tank. This section also features the factorial experimental design and procedure of the experiment in this study.

2.1 Turbine-like mechanical fan

This study employs a simplified model of a turbine, called turbine-like, by using a mechanical fan. The rotating blades of the fan were expected to represent a similar conversion process of the stream energy to mechanical energy in a turbine. Attached to the inlet part of the fan was the developed turbulence generator. **Figure 1** shows the simplified image of the mechanical fan with the attached turbulence generator. As shown in **Figure 1**, a turbulence generator is placed in front of the center of the mechanical fan and facing the incoming stream to the fan. The turbulence generator has a hemisphere shape, which is determined by its diameter, D_T , and maximum length, L_T . The curvature of the turbulence generator is not optimized yet in this study. The figure also depicts another important parameter of the distance between the turbulence generator to the inlet of the mechanical fan, s_T .

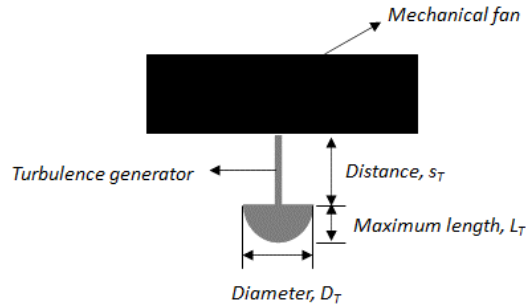


Fig. 1. Simplified image of the passive turbine-like mechanical fan

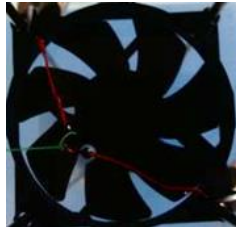


Fig. 2. Brushless DC axial fan

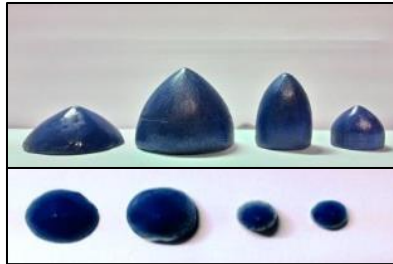


Fig. 3. Developed passive turbulence generators. Top: front view, Bottom: top view

The mechanical fan, as shown in **Figure 2**, was a standard seven (7) blades 12 V brushless DC axial fan for cooling equipment in a personal computer (PC) case. The fan has a diameter, D_F , of 0.08 m and a height, h_F , of 0.025 m. There were four types of turbulence generators in this study, as shown in **Figure 3**. The figure presents the front and top views of the turbulence generators to show the contribution of diameter and maximum length to the shape of the turbulence generator. The turbulence generators were made from painted Akasia Wood.

2.2 Sinking test

To observe the effect of the turbulence generator on the rotational speed of the fan, this study employs a simple sinking test in a water tank. The water tank can be seen in **Figure 4**. The tank has a dimension of 0.30 m × 0.30 m × 0.50 m for the length, width, and depth, respectively. The figure also depicts the initial position of the observed system, a fan rail, and the bottom pad of the tank. The sinking test involved a translational motion of the mechanical

fan from the top surface (initial position) to the bottom of the water-filled tank. In this way, the translation of the fan induces a stream to the blades. The stream generates forces to rotate the blades of the fan, thus creating a pressure difference within the fan and thrust force in the direction of the translation motion. The faster the rotational speed of the blades generates a higher force, the faster the fan reaches the bottom side of the tank. The mass of the turbulence generator could be ignored since the mass of the developed turbulence generator is relatively small compared to the mass of the fan.

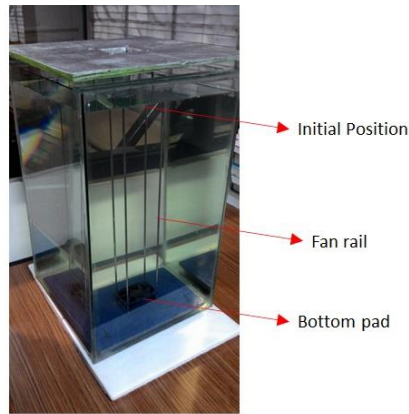


Fig. 4. Water tank for sinking test

2.3 Factorial Experimental Design

This study employs a full factorial design method to measure response combinations of factor levels [16, 17]. The method was considering several factors to study the interaction effect of factors and determine which is the most significant factor [18, 19]. It could estimate separately the main effect and their higher-order interactions. This method should support the main objective of this study to obtain the highest significance factor of the turbulence generator that contributes to the turbine-like performance in a low-speed flow regime. The full factorial design in this study involved three factors at two levels. The three factors were diameter, D_T , maximum length, L_T , and the distance between the back side of the turbulence generator to the front side of the mechanical fan, s_T . The two levels were marked as “+” and “-“. A full factorial design that contains all possible combinations of low/high levels for all the factors is tabulated in Table 1. The yield of the study is Submerged time, T , which is counted by using a digital stopwatch.

Table 1. Full factorial design for experimental activities.

Factors Studied	Value	Sign
Diameter of turbulence generator, D_T [m]	0.02	-
	0.04	+
Maximum length of turbulence generator, L_T [m]	0.02	-
	0.04	+
Turbulence generator distance, s_T [m]	0.02	-
	0.04	+

This study employs the Yates algorithm to find the main effects and the interaction effects. The algorithm generates least squares estimates for factor effects for all factors and all relevant interactions and tests the significance of effect estimates. The algorithm utilizes a specific arrangement of experiment data called the Yates order. The experiments with three ($k = 3$) factors were arranged with each factor in its own column, $2^{(k-1)}$ minus signs in a column (low levels) and followed by the same number of plus signs (high levels). The matrix of experimental running for a full factorial design with two levels and three factors is presented in Table 2.

Table 2. Yates order of the full factorial design with three factors.

Experimental Running			
No	D_T	L_T	s_T
1	-	-	-
2	+	-	-
3	-	+	-
4	+	+	-
5	-	-	+
6	+	-	+
7	-	+	+
8	+	+	+

2.3 Experimental Procedure

The initial stage of the experimental activities consists of the preparation of experimental equipment and measuring the initial depth of water in the tank. The equipment included a water-filled water tank, turbulence generators, a mechanical fan, a digital stopwatch, a ruler, and a computer as a data processor. The main experimental activities can be seen schematically in **Figure 5**. As shown in the diagram, each combination in Yates Order was repeated three times to obtain the average values of the measurement. The recorded submerged time, T , and traveled distance of the mechanical fan, s , will be used to calculate the sinking speed, V , of the mechanical fan as expressed by

$$V = \frac{s}{T} \quad (1)$$

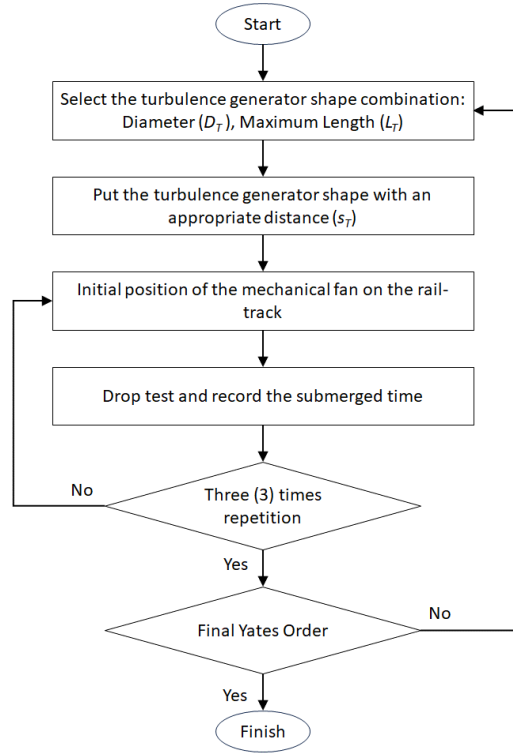


Fig. 5. Schematic diagram of the main experimental activities.

3 Results and Discussion

The experimental activities were performed according to the procedure in the previous section. The measurement presents the submerged times as the yield of the influence factor. Experimental data of the present study, based on the Yates Order, is presented in Table 3. The sinking speed of the mechanical fan was calculated by using equation (1). The result of sinking speed, V , indicates the arrangement in No. 5 achieves the maximum sinking speed of 0.44 m/s , while the arrangement in No. 4 gets the minimum sinking speed of 0.26 m/s . The sinking speed data can be arranged three-dimensionally as vertices of a cube plot, as can be seen in Figure 6. In the figure, the maximum sinking speed is in the left-back vertices of the bottom side of the cube. The placement indicates that it occurs at the combination of a low level of D_T , a low level of L_T , and a high level of s_T . The minimum sinking speed is in the right-front vertices of the top side of the cube. The placement indicates that it occurs at the combination of a high level of D_T , a high level of L_T , and a low level of s_T .

Table 3. The sinking speed of the turbine-like mechanical fan.

No	Submerged Time, T [s]			Average Time, T_{avg} [s]	Distance, s [m]	Sinking Speed, V [m/s]
	1	2	3			

1	1.19	1.19	1.13	1.17	0.375	0.32
2	1.03	0.99	1.08	1.03	0.375	0.36
3	1.11	1.09	1.05	1.08	0.355	0.33
4	1.38	1.41	1.33	1.37	0.355	0.26
5	0.80	0.79	0.81	0.80	0.355	0.44
6	0.88	0.90	0.86	0.88	0.355	0.40
7	0.91	0.91	0.89	0.90	0.335	0.37
8	0.86	0.88	0.88	0.87	0.335	0.38

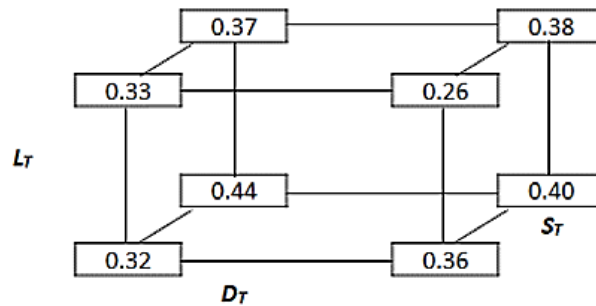


Fig. 6. Cube plot of the sinking speed of the mechanical fan.

The calculation of the effects of factors by using Yates Algorithm is presented in Table 4. As shown in the table, the column "Effect" contains the list of main effects and interactions from the factorial experiment in standard order. The values of the measurement results in Yates order are placed in the column " V [m/s]". The first four values in column "1" are obtained by summing the adjacent pairs of sinking speed values, while the second four values in column "1" are obtained by subtracting the same adjacent pairs of the sinking speed values. The values in column "2" are summing and subtracting from the adjacent values from column "1". Further, the values in column "3" are computed using adjacent values from column "2". The values in column "Estimate" are obtained by dividing the values in column "3" by divisor values. The values on the Estimates column in **Table 4** should be ordered sequentially to match the normal probability values of the effects. The ordered sequence can be seen in Table 5.

Table 4. Effect of factor by using Yates Algorithm.

No	D_r [m]	L_r [m]	s_r [m]	V [m/s]	V^2	1	2	3	3^2	Divisor	Estimates	Effect
1	0.02	0.02	0.02	0.32	0.10	0.68	1.27	2.87	8.24	8	0.3589	Average
2	0.04	0.02	0.02	0.36	0.13	0.59	1.60	-0.05	0.00	4	-0.0136	1
3	0.02	0.04	0.02	0.33	0.11	0.85	-0.03	-0.19	0.04	4	-0.0475	2
4	0.04	0.04	0.02	0.26	0.07	0.75	-0.03	-0.06	0.00	4	-0.0146	12
5	0.02	0.02	0.04	0.44	0.20	0.04	-0.10	0.33	0.11	4	0.0830	3

6	0.04	0.02	0.04	0.40	0.16	-0.07	-0.09	0.00	0.00	4	-0.0002	13
7	0.02	0.04	0.04	0.37	0.14	-0.04	-0.11	0.00	0.00	4	0.0011	23
8	0.04	0.04	0.04	0.38	0.15	0.01	0.05	0.16	0.03	4	0.0412	123

Table 5. Ordered sequence of the estimates of the factors.

Order Number, <i>l</i>	1	2	3	4	5	6	7
Effect	-0.0475	-0.0146	-0.0136	-0.0002	0.0011	0.0412	0.0830
Identity of effect	2	12	1	13	23	123	3
P = 100×(I-0.5)/7	7.14	21.43	35.71	50.00	64.29	78.57	92.86

Standard error of the main effects, *SE*, can be determined by using estimates data of the interaction effects e.g., 12, 13, 23 and 123.

$$SE^2 = \frac{1}{4}\{-0.0146^2 + (-0.0002)^2 + 0.0011^2 + 0.0412^2\} = 0.00048$$

$$SE = 0.022$$

The standard error of the main effect and the estimated effects with standard error can be seen in Table 6 and Table 7, respectively. From the standard error data, in the assumption of normal distribution, reference t_v distribution with 4 degrees of freedom can be produced. By using this assumption, 95% of the distribution would be within an interval of $\pm t_{4,0.025} \times SE = \pm 2.776 \times 0.022 = 0.061$.

Table 6. Standard error of the main effect.

Standard Error, SE			
SE^2	SE	$t_{(4, 0.025)}$	+/-
0.00048	0.022	2.776	0.061

Table 7. Estimated effects with standard error.

Effects	Estimates ± Standard Error
Average	0.3589 ± 0.011
1	-0.0136 ± 0.022
2	-0.0475 ± 0.022
3	0.0830 ± 0.022
12	-0.0146
13	-0.0002
23	0.0011
123	0.0412

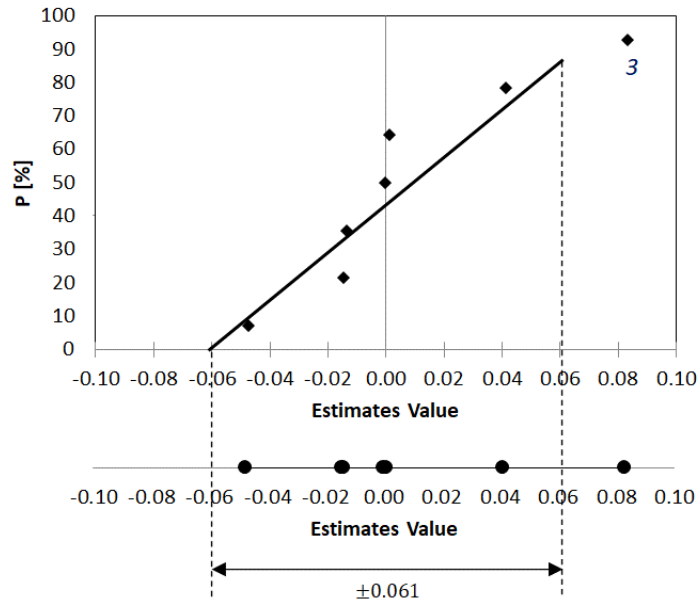


Fig. 7. Probability plot and dot diagram of the Estimates values.

The normal probability plot and dot diagram of the “Estimates” values can be seen in **Figure 7**. Highly likely that the main effect “Estimates” of 3 (turbulence generator distance, s_T) represent real effects, following the results in [10, 11]. Since 95% of the distribution would be contained within the interval ± 0.061 , the effect of s_T as the significant factor should be less noise. An increase in distance, s_T , from 0.02 m to 0.04 m increases the sinking speed by 0.083 m/s and the effect is consistent over the levels of the other factors tested. This result also supports the relation between maximum and minimum sinking speeds to the turbulence generator distance in the Cube Plot.

4 Conclusion

A simple passive turbulence generator potentially enhances the rotational speed of the turbine blades in low-speed flow. Factorial design with the Yates algorithm has been implemented to obtain the main effect and interaction effect of the turbulence generator shapes to the rotational speed of the turbine-like fan. The distance of the turbulence generator (s_T) is the significant factor within the significant level of 0.05, degree of freedom of 4, and t-value of 2.776. Further development could include the evaluation of more detailed fluid physics phenomena due to the turbulence generator with a numerical method such as Computational Fluid Dynamics. Another possible development is the development of a prototype of the turbine with an actively controlled turbulence generator, especially in the distance parameter.

Acknowledgments.

We would like to thank Universitas Pertamina for the academic and technical support.

References

- [1] Akin-Ponnle, A. E., Pereira, F. S., Madureira, R. C. & Carvalho, N. B. From Macro to Micro: Impact of Smart Turbine Energy Harvesters (STEH), on Environmental Sustainability and Smart City Automation. *Sustain.* **14**, (2022).
- [2] Rakibuzzaman, M., Suh, S. H., Kim, H. H., Ryu, Y. & Kim, K. Y. Development of a hydropower turbine using seawater from a fish farm. *Processes* **9**, 1–24 (2021).
- [3] Qian, G. W. & Ishihara, T. Numerical study of wind turbine wakes over escarpments by a modified delayed detached eddy simulation. *J. Wind Eng. Ind. Aerodyn.* **191**, 41–53 (2019).
- [4] Porté-Agel, F., Bastankhah, M. & Shamsoddin, S. *Wind-Turbine and Wind-Farm Flows: A Review. Boundary-Layer Meteorology* vol. 174 (Springer Netherlands, 2020).
- [5] Ashglaf, M., Nichita, C. & Dakyo, B. Control Strategies Design for a Small-Scale Wind Turbine with a Doubly Fed Induction Generator. *7th Int. IEEE Conf. Renew. Energy Res. Appl. ICRERA 2018* 1092–1097 (2018) doi:10.1109/ICRERA.2018.8566836.
- [6] Ye, D. X., Lai, X. D. & Li, H. PIV measurement and study on turbulence generator flow field of medium consistency pump. *IOP Conf. Ser. Earth Environ. Sci.* **163**, (2018).
- [7] Fragner, R., Mazellier, N., Halter, F., Chauveau, C. & Gökalp, I. Multi-scale high intensity turbulence generator applied to a high pressure turbulent burner. *Flow, Turbul. Combust.* **94**, 263–283 (2015).
- [8] Feng, J., Acton, M., Baglietto, E., Kraus, A. R. & Merzari, E. On the relevance of turbulent structures resolution for cross-flow in a helical-coil tube bundle. *Ann. Nucl. Energy* **140**, 107298 (2020).
- [9] Li, H., Zhuang, H. & Geng, W. Design of a turbulence generator of medium consistency pulp pumps. *Int. J. Rotating Mach.* **2012**, (2012).
- [10] Jin, Y., Liu, H., Aggarwal, R., Singh, A. & Chamorro, L. P. Effects of freestream turbulence in a model wind turbine wake. *Energies* **9**, (2016).
- [11] Baloutaki, M.A., Carriveau, R., Ting, D.S.K. Performance of a vertical axis wind turbine in grid generated turbulence. *Sustainable Energy Technologies and Assessments*, **11**, 178-185 (2015). <https://doi.org/10.1016/j.seta.2014.12.007>
- [12] Schubel, P. J. & Crossley, R. J. Wind turbine blade design. *Energies* **5**, 3425–3449 (2012).
- [13] Tran, D. H., Sareni, B., Roboam, X. & Espanet, C. Integrated optimal design of a passive wind turbine system: An experimental validation. *IEEE Trans. Sustain. Energy* **1**, 48–56 (2010).
- [14] Ahmad, M., Abdul Aziz, M., Mior Ahmad Khushairi, M. & Mazrul Nizam, A. Application Of Factorial Design To The Stress Phenomenon Of Bacillus Cereus (Atcc 14579) Growth. *Aust. J. Basic Appl. Sci.* **10**, 148–156 (2016).
- [15] Bahçecitapar, M. K. Estimation of sample size and power for general full factorial designs. *İstatistikçiler Dergisi İstatistik ve Aktüerya* **9**, 79–86 (2016).
- [16] Oliveira, M. de, Lima, V. M., Yamashita, S. M. A., Alves, P. S. & Portella, A. C. Experimental Planning Factorial: A brief Review. *Int. J. Adv. Eng. Res. Sci.* **5**, 166–177 (2018).
- [17] Özbay, N., Yargıç, A. Ş., Yarbay-Şahin, R. Z. & Önal, E. Full factorial experimental design analysis of reactive dye removal by carbon adsorption. *J. Chem.* **2013**, (2013).
- [18] Raison, M. & Mark, F. Z. Application of two-level full factorial design and response surface methodology in the optimization of inductively coupled plasma-optical emission spectrometry (ICPOES) instrumental parameters for the determination of platinum. *J. Geol. Min. Res.* **9**, 43–53 (2017).
- [19] Bingham, D., Sitter, R., Kelly, E., Moore, L., & Olivas, J. D. Factorial Designs with Multiple Level of Randomization. *Statistica Sinica*, **18**, 2, 493–513 (2008). <http://www.jstor.org/stable/24308492>